Influence of the Crystallization Solvent on Molecular and Supramolecular Structures of Silver(I) Tris(3-Phenylpyrazolyl)methane Complexes

Daniel L. Reger,*[a] Radu F. Semeniuc,[a] and Mark D. Smith[a]

Keywords: N ligands / Solvent effects / Noncovalent interactions / Silver / Supramolecular chemistry

The compound [{HC(3-Phpz)$_3$}Ag](BF$_4$) (pz = pyrazolyl ring) has been prepared and shown to crystallize in four different forms depending on the solvent. Vapor-phase diffusion of diethyl ether into nitromethane solutions of the complex produces two polymorphs, an orthorhombic form (**1**) and triclinic form (**2**). Both polymorphs are coordination polymers constructed by a κ^2–κ^1 coordination of the tris(3-Phpz)methane units and have similar, but different, supramolecular structures. In **1** there are two independent chains linked by C–H···π interactions. In **2** only one type of chain is present, with a different internal structure than in **1**. Non-covalent forces, mainly C–H···π interactions, organize the chains into sheets and the sheets into a final 3-D supramolecular structure in the case of **1**, while in the case of **2** only a 2-D supramolecular structure forms. In contrast, vapor-phase diffusion of diethyl ether into acetonitrile or acetone solutions produces [{HC(3-Ph-pz)$_3$}Ag{(CH$_3$)$_2$CO}](BF$_4$) (**3**) and [{HC(3-Phpz)$_3$}-Ag{CH$_3$CN}](BF$_4$) (**4**). In these compounds, the ligand shows tripodal coordination to a single silver center and coordination of one solvent molecule to the metallic center. Both compounds form 3-D supramolecular structures organized by both C–H···π interactions and weak C–H···F hydrogen bonds and in the case of **4** π–π stacking.

Introduction

In 1966 Trofimenko introduced the tripodal hydrotris(pyrazolyl)borate family of ligands. They remain an important class of N_3 tripodal ligands in many fields of coordination chemistry, supramolecular chemistry, and catalysis.[1−5] Substituted hydrotris(pyrazolyl)borates, especially in the 3-position of the pyrazolyl ring, offer the possibility of controlling steric factors, making them suitable ligands in various enzyme models.[6−9] We have recently been investigating the isoelectronic tris(pyrazolyl)methane ligands and wish to demonstrate the ability of these neutral ligands to control the coordination chemistry of various metals through careful choice of substituents on the pyrazolyl rings.[10−15] With silver(I), we have reported the solid-state structures of [{HC(3,5-Me$_2$pz)$_3$}$_2$Ag](O$_3$SCF$_3$), [{HC(3-Butpz)$_3$}Ag](O$_3$SCF$_3$), and [{HC(3-Butpz)$_3$}Ag(CNBut)](O$_3$SCF$_3$).[12] Recently, others reported a series of silver derivatives of simple tris(pyrazolyl)methane ligands[16] and structures based on linking pyrazolyl rings with organic spacers.[17,18]

We have expanded the chemistry of simple tris(pyrazolyl)-methane ligands with the synthesis of a new class of multitopic ligands of the general formula C_6H_{6-n}[CH$_2$OCH$_2$C(3-Rpz)$_3$]$_n$, (R = H or Ph, n = 2, 4). These ligands are based on semi-rigid organic spacers that link two or more tris(pyrazolyl)methane units in a single molecule.[19−25] We have shown that metal complexes of these ligands form an array of unusual supramolecular structures supported by a multitude of non-covalent interaction, such as weak hydrogen bonds,[19−22] intermolecular[20,25] or intramolecular[22,24] π−π stacking, and C−H···π interactions.[20,24,25] This versatility is a consequence of the presence of the aromatic pyrazolyl rings and linking arene rings that can act as acceptors in C−H···π interactions or participate in π−π stacking. Another factor is that the hydrogen atoms within the pyrazolyl rings are acidic enough to be involved in weak hydrogen bonds. Additional structural diversity is derived from the ability of the tris(pyrazolyl)methane units to act as (a) a κ^3-tripodal ligand, (b) a κ^2-ligand, with the third pyrazolyl not coordinated to a metal, and (c) a bridge between two metals in a $\kappa^2-\kappa^1$ coordination mode, see Scheme 1. We defined these ligands as *structurally adaptive*.[24,25] A structurally adaptive ligand can adjust its shape to maximize covalent and non-covalent interactions and the overall structure of the supramolecular array will be the resultant of the interplay amongst all forces. While rigid ligands allow a better prediction of the overall structure, shape and porosity of the resulting array,[26,27] these semi-rigid, structurally adaptive ligands offer new insights into the self-assembly process. For example, [*o*-C$_6$H$_4${CH$_2$OCH$_2$C(3-Phpz)$_3$}$_2$Ag$_2$(BF$_4$)$_2$]$_n$ forms a 1-D organometallic coordination polymer that contains two different types of silver(I) cations arranged in bimetallic units. The bimetallic units show three different types of bridging

[a] Department of Chemistry and Biochemistry University of South Carolina,
Columbia South Carolina 29208, USA
Fax: (internat.) +1-803/777-9521
E-mail: Reger@mail.chem.sc.edu

Supporting information for this article is available on the WWW under http://www.eurjIc.org or from the author.

  DOI: 10.1002/ejic.200300141

interactions, including a $\kappa^2-\kappa^1$ coordination mode of a tris(3-Ph-pyrazolyl)methane unit, a silver η^2-bonded to a phenyl group and $\pi-\pi$ stacking interactions.[23]

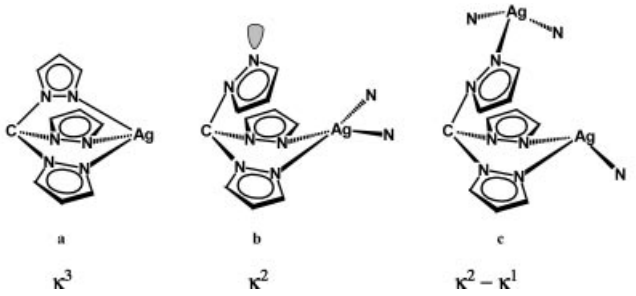

Scheme 1. Observed coordination modes of the $[HC(pz)_3]$ unit in silver(I) chemistry: a) κ^3 — tripodal; b) κ^2 — chelating one metal with the third pyrazolyl ring not coordinated; c) $\kappa^2-\kappa^1$ — bridging two metallic centers

In an attempt to elucidate the intimate processes that lead to the formation of these supramolecular species containing multitopic tris(pyrazolyl)methane ligands, we focused our attention back on simple tris(pyrazolyl)methane ligands, ligands that have the same potential to enter into non-covalent interactions and poses the same structural diversity in the modes of covalent bonding, to study the molecular and supramolecular structures of complexes of the tris(pyrazolyl)methane unit without the organizational feature of the linking, semi-rigid organic spacer. We have shown that $[\{HC(pz)_3\}CuPPh_3](NO_3)$ and $[\{HC(3\text{-}Phpz)_3\}CuPPh_3](NO_3)$ form a two dimensional supramolecular network of dimeric units.[28] Reported here are the synthesis and spectral characterization of $[\{HC(3\text{-}Phpz)_3\}_2Ag](BF_4)$, and the solid state structures of four different crystallographic forms of the complex with emphasis on the importance of the crystallization solvent and the role played by the counterion in influencing the types of covalent and non-covalent forces that organize the supramolecular networks.

Results and Discussion

Syntheses and Characterization

$HC(3\text{-}Phpz)_3$ was prepared in high yield using a modified procedure of the published preparation[13] that avoids the chromatography step. The compound $[\{HC(3\text{-}Phpz)_3\}Ag](BF_4)$ (Scheme 2) was prepared by mixing a THF solution of the ligand with a THF solution of $AgBF_4$ in a 1:1 ratio. The same product is formed in a reaction using a 1:2 metal to ligand ratio, with one equivalent of the ligand recovered from the filtrate. The compound is an air and light stable solid. It is soluble in acetone, acetonitrile, and nitromethane but insoluble in halogenated solvents, water, or alcohols.

The ^1H NMR spectrum of the solid in CD_3CN shows that the acetonitrile completely replaces the ligand in solution; the spectrum of the compound in CD_3CN is the same as the free ligand in this solvent. However, the ^1H NMR spectra of the compound in deuterated acetone or nitromethane are clearly different from the free ligand, showing the coordination of the ligand to the silver(I) in these solutions. Although the X-ray structures of all crystalline forms of $[\{HC(3\text{-}Phpz)_3\}Ag](BF_4)$ show that in the solid state the pyrazolyl rings are non-equivalent (vide infra), the NMR spectra of $[\{HC(3\text{-}Phpz)_3\}Ag](BF_4)$ and similar complexes of silver containing the $[C(pz)_3]$ unit[20,21,23,25] all show equivalent rings, presumably because of fast exchange of the ligands and metals on the NMR timescale. This fast exchange process is maintained even at low temperatures.

An interesting solvent dependence was observed in the chemical shifts of the hydrogen atoms of the silver complex when they were compared with their initial position in the free ligand. In deuterated acetone the resonances that corresponds to the methine hydrogen and the 5-H (pz) were shifted ca. 0.4 ppm while the other resonances [the 4-H(pz) and phenyl hydrogens] were found at almost the same positions as in the free ligand. In deuterated nitromethane the only peak that was found shifted significantly was the 5-H(pz) with a shift of ca. 0.25 ppm. The greater shifts in acetone are likely due to hydrogen bonding of the acetone with the acidic methine hydrogen, an effect that has been observed previously.[29,30]

Electrospray mass spectroscopy (ES/MS) has emerged as a technique for investigating solution aggregation of covalent and noncovalent species. In the case of coordination polymers, ES/MS was used to probe the aggregation between the ligands and silver(I) salts in solution, aggregates that might be related to the building blocks and subsequently to the final supramolecular structure of the coordination polymers.[31] We performed the ES/MS experiment in three different solvents to establish such a connection,

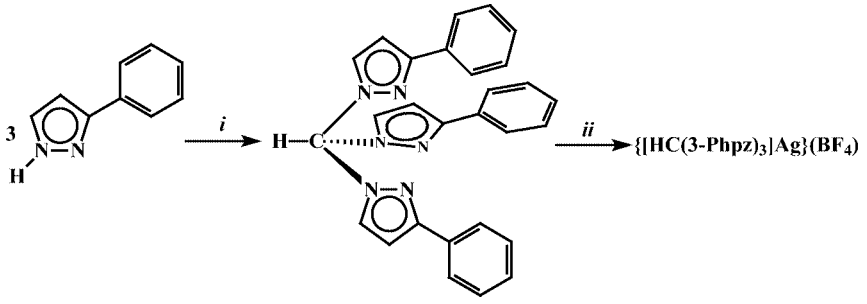

Scheme 2. Preparation of $[\{HC(3\text{-}Phpz)_3\}Ag](BF_4)$: i: $HCCl_3$, Na_2CO_3, nBu_4NBr; ii: $AgBF_4$, THF

especially given the important influence the crystallization solvent has over the solid state structures (vide infra).

In nitromethane, four peaks were identified at 551, 610, 991, and 1187 *m*/*z*, corresponding to $[LAg]^+$, $[LAg(nitromethane)]^+$, $[L_2Ag]^+$, and $[L_2Ag_2(BF_4)]^+$ respectively. The spectrum is presented in Figure 1. The most abundant peak is the one that corresponds to $[LAg]^+$ species. The least abundant peak corresponds to the species that contains two ligands, two silver(I) ions and one BF_4^-, a peak that presumably arises from a species related to the presence of a coordination polymer in solution. When acetone was used, three peaks were identified at 551, 607, and 991 *m*/*z*, corresponding to $[LAg]^+$, $[LAg(acetone)]^+$, and $[L_2Ag]^+$ respectively. In this case the most abundant peak is the one that corresponds to the $[LAg(acetone)]^+$ species. The same situation was observed when acetonitrile was used as solvent. Three peaks at 551, 590, and 991 *m*/*z* were observed, corresponding to $[LAg]^+$, $[LAg(acetonitrile)]^+$, and $[L_2Ag]^+$ respectively. Interestingly, the most abundant species observed here is the one that corresponds to $[L_2Ag]^+$ species. These $[L_2Ag]^+$ species in all solvents could indicate individual species with a metal to ligand ratio of 1:2 in solution, but given that such species have only been observed for $[\{\kappa^3\text{-HC(3,5-Me}_2\text{pz)}_3\}_2\text{Ag}]^+$ [12] they more likely arise from solution coordination polymers. While the observation of $[L_2Ag_2(BF_4)]^+$ in the spectrum taken from the non-coordinating solvent nitromethane almost certainly arises from a solution coordination polymer, further studies are needed to definitively establish the relationship between ES/MS results and solution aggregation. What is clear from the NMR and ES/MS studies and the fact that coordination compounds of the ligand crystallize from acetonitrile and acetone (vide infra) is that in solutions of coordinating solvents a complicated series of equilibria take place between $[LAg]^+$ species (either aggregated or not), and species in which the solvent has partially or completely displaced the ligands.

Solid-State Studies

Given the versatility of the tris(3-Ph-pyrazolyl)methane ligand (L) we determined the solid state structure of the free ligand for comparison purposes. The molecular structure of the ligand together with the crystallographic and structure refinement data and selected bond lengths and angles are presented as supplementary information (Figure S1 and Tables S1 and S2, Supporting Information, see footnote on page 1 of this article). The ligand structure consists of discrete molecules without significant intermolecular associations. The orientation of the three pyrazolyl rings is a propeller arrangement with only one of the donor nitrogen atoms oriented toward the potential bonding "pocket" of the ligand. The pyrazolyl and phenyl rings are not in the same plane, the N(*n*1)−C(*n*1)−C(*n*4)−C(*n*5) (where *n* denotes the ring number) torsion angles between the rings ranging from 155 to 172 degrees.

We have grown crystals of $[\{HC(3\text{-Phpz})_3\}Ag](BF_4)$ from vapor phase diffusion of diethyl ether into nitromethane, acetonitrile, and acetone solutions of the complex in order

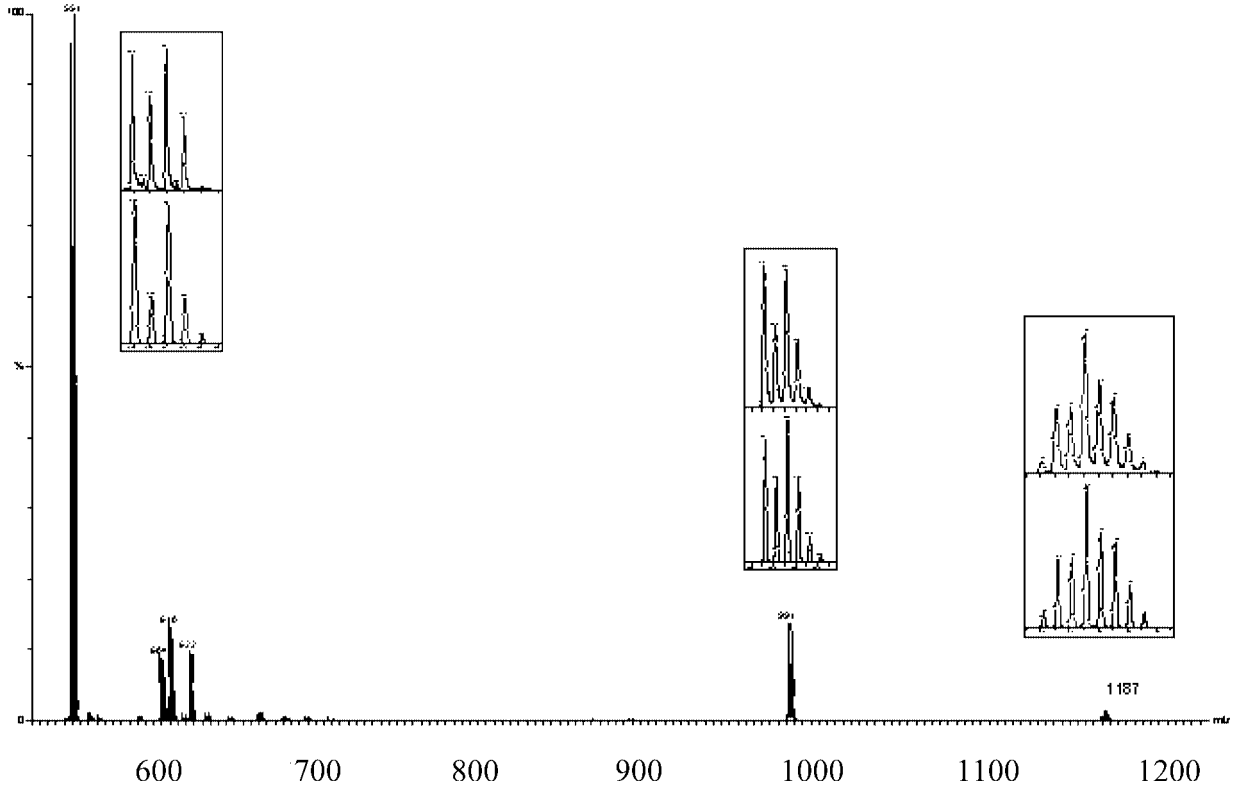

Figure 1. Portion of ES/MS spectra of $[\{HC(3\text{-Phpz})_3\}Ag](BF_4)$ in nitromethane; the insets show the observed (top) and calculated (bottom) isotopic patterns

to ascertain the effects of non-coordinating and coordinating solvents on molecular and the subsequent supramolecular structures. When nitromethane was used, two polymorphs were found, an orthorhombic form (**1**) and triclinic form (**2**). Both polymorphs are coordination polymers constructed by a κ^2-κ^1 coordination of the tris(3-Ph-pyrazolyl)methane units, with a metal to ligand ratio of 1:1. In contrast, when acetonitrile or acetone was used, two new discrete compounds were obtained, with the same metal to tris(pyrazolyl)methane ligand ratio, of the formula [{HC(3-Phpz)$_3$}Ag{$(CH_3)_2CO$}](BF_4) (**3**) and [{HC(3-Phpz)$_3$}Ag{CH_3CN}](BF_4) (**4**). In these compounds, the ligand shows tripodal coordination to a single silver center. In addition one solvent molecule is coordinated to the metallic center. The metrical parameters for all four compounds (bond lengths and angles) are given in Table 1.

The two crystallographically independent [{HC(3-Phpz)$_3$}Ag]$^+$ units and two BF_4^- anions of **1** are pictured in Figure 2 (a and b) together with their partial crystallographic numbering scheme (for a full crystallographic numbering scheme see the ORTEP representation of **1** in the Supplementary Information, Figure S2). Each ligand is κ^2-κ^1 coordinated to silver(I) centers. The polyhedra about Ag(1) and Ag(2) atoms are flattened trigonal pyramids [sum of the N−Ag−N bond angles = 332° for Ag(1) and 341° for Ag(2)], with a large distortion caused by the restricted bite angle [82.55(11)° for Ag(1) and 84.11(10)° for Ag(2)] of the κ^2-bonded ligand. The BF_4^- anions are located along the polymeric strand in the vicinity of the silver atoms. There are several close contacts between the silver and fluorine atoms in both chains, interactions that are best described as secondary bonds.[32] The Ag···F distances, shown as blue dotted lines in Figure 2, are listed in Table 2, together with other non-covalent parameters for **1**.[33−37] Interestingly, in **1** the BF_4^- anions are not involved in the organization of the extended structure, a structural feature frequently observed with other similar complexes.[21,23,25] There are several C−H···F weak hydrogen bonds (see Table 2), but they are interstrand only and pictured in Figure 2 (a and b) also as blue dotted lines. The H···F distances are all well below the sum of van der Waals radii for hydrogen and fluorine and are typical for this type of hydrogen bonding.

Table 1. Selected bond lengths and angles for **1**−**4**

1			
Ag(1)−N(11)	2.381(3)	N(11)−Ag(1)−N(21)	82.55(11)
Ag(1)−N(21)	2.304(3)	N(11)−Ag(1)−N(31)′	111.52(11)
Ag(1)−N(31)′	2.255(3)	N(21)−Ag(1)−N(31)′	137.59(10)
Ag(2)−N(41)	2.379(3)	N(41)−Ag(2)−N(51)	84.11(10)
Ag(2)−N(51)	2.294(3)	N(41)−Ag(2)−N(61)′	117.38(10)
Ag(2)−N(61)′	2.230(2)	N(51)−Ag(2)−N(61)′	139.13(11)
2			
Ag(1)−N(11)	2.324(3)	N(11)−Ag(1)−N(61)	140.11(10)
Ag(1)−N(21)	2.353(3)	N(21)−Ag(1)−N(61)	112.61(10)
Ag(1)−N(61)	2.221(3)	N(11)−Ag(1)−N(21)	86.08(9)
Ag(2)−N(31)′	2.217(3)	N(31)′−Ag(2)−N(41)	145.96(10)
Ag(2)−N(41)	2.255(3)	N(31)′−Ag(2)−N(51)	111.54(10)
Ag(2)−N(51)	2.479(3)	N(41)−Ag(2)−N(51)	85.17(9)
3			
Ag(1)−N(111)	2.412(3)	O(101)−Ag(1)−N(131)	138.57(12)
Ag(1)−N(121)	2.381(3)	O(101)−Ag(1)−N(121)	123.95(12)
Ag(1)−N(131)	2.338(3)	N(131)−Ag(1)−N(121)	79.48(11)
Ag(1)−O(101)	2.231(3)	O(101)−Ag(1)−N(111)	131.25(12)
Ag(2)−N(211)	2.358(3)	N(131)−Ag(1)−N(111)	82.00(11)
Ag(2)−N(221)	2.413(3)	N(121)−Ag(1)−N(111)	80.46(11)
Ag(2)−N(231)	2.363(3)	O(201)−Ag(2)−N(211)	135.12(12)
Ag(2)−O(201)	2.172(4)	O(201)−Ag(2)−N(231)	123.60(13)
		N(211)−Ag(2)−N(231)	83.19(11)
		O(201)−Ag(2)−N(221)	133.98(12)
		N(211)−Ag(2)−N(221)	81.95(10)
		N(231)−Ag(2)−N(221)	78.74(10)
4			
Ag(1)−N(111)	2.337(2)	N(101)−Ag(1)−N(111)	132.15(8)
Ag(1)−N(121)	2.4047(19)	N(101)−Ag(1)−N(131)	131.32(8)
Ag(1)−N(131)	2.353(2)	N(111)−Ag(1)−N(131)	80.34(7)
Ag(1)−N(101)	2.137(2)	N(101)−Ag(1)−N(121)	132.63(8)
Ag(2)−N(211)	2.3549(18)	N(111)−Ag(1)−N(121)	78.73(7)
Ag(2)−N(221)	2.394(2)	N(131)−Ag(1)−N(121)	81.13(7)
Ag(2)−N(231)	2.361(2)	N(201)−Ag(2)−N(211)	136.49(8)
Ag(2)−N(201)	2.149(2)	N(201)−Ag(2)−N(231)	133.62(8)
		N(211)−Ag(2)−N(231)	81.89(7)
		N(201)−Ag(2)−N(221)	123.46(8)
		N(211)−Ag(2)−N(221)	78.63(6)
		N(231)−Ag(2)−N(221)	81.82(7)

There are two crystallographically independent chains (Figure 2, c and e), that run along the *a* axis, associated with the independent atoms Ag(1) and Ag(2). As pictured in Figure 2 (c), the chain associated with Ag(1) has an intrastrand π−π stacking interaction (black double dotted lines) between the [N(31)−N(32)−C(31)−C(32)−C(33)] pyrazole ring that is κ^1 coordinated to silver(I) and the [C(14)−C(15)−C(16)−C(17)−C(18)−C(19)] phenyl ring attached to the [N(11)−N(12)−C(11)−C(12)−C(13)] pyrazolyl ring that is κ^2 coordinated to the same silver. The two rings are parallel displaced, resulting in a centroid−centroid distance of 3.83 Å, but with a perpendicular distance between the rings of 3.47 Å. These values are typical for a π−π stacking interaction.[35] There is no similar interaction in the chains associated with Ag(2). Figure 2 (d and f) show a view of both chains along the *a* axis, illustrating the overall similarity in the chains, where the only important difference is the orientation of the phenyl rings involved in the π−π stacking in the Ag(1) chain.

These non-covalent forces appear to be correlated with a twisting of the pyrazolyl rings. For maximum overlap with the lone pair on the donor nitrogen atoms the metal would lie in the plane of each pyrazole ring. Any deviation where the metal lies out of this plane can be measured by the Ag−N(*n*1)−N(*n*2)−C(*n*1) (where *n* denotes the ring number) torsion angle, an angle that is 180° for a metal located in the same plane as the ring. We have shown[38] that these deviations are related to the size of the metal when the tris(pyrazolyl)methane ligand is tripodal. For **1**, where the ligand is not tripodal, the angles associated with the Ag(1) chain are 160°, 145°, and 122° and those associated with Ag(2) chain are 165°, 143°, and 134° respectively. The greatest value (least twisting) in this series (165°) is correlated with a pyrazolyl and its associated phenyl ring that are *not*

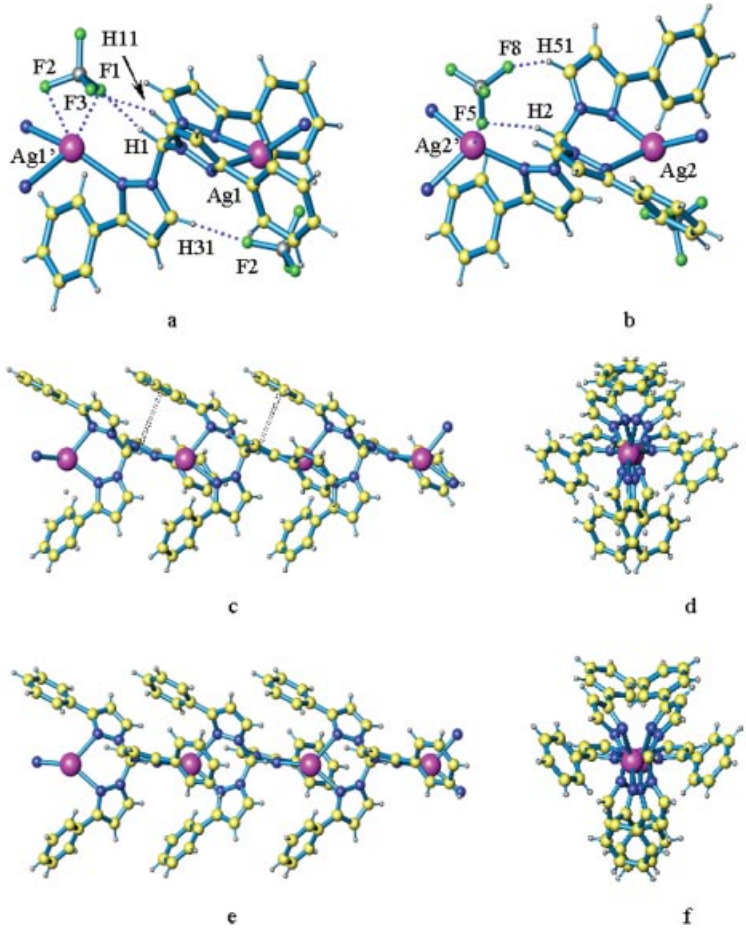

Figure 2. a, b) Formation of the two independent chains in **1** based on the κ^2-κ^1 coordination mode of the HC(3-Phpz)$_3$ ligand; secondary Ag···F bonds and C−H···F weak hydrogen bonds are shown as blue dotted lines; color scheme: silver purple, carbon yellow, nitrogen blue, fluorine green; c) Ag(1) chain with the π−π stacking between pyrazolyl and phenyl rings showed as black double dotted lines; d) end-on view of the same chain; e) Ag(2) chain, with no intrastrand interactions; f) view down the Ag(2) chain

involved in any non-covalent interaction. In contrast, the smallest value in this series (122°) is related to the [N(11)−N(12)−C(11)−C(12)−C(13)] pyrazolyl ring that has its associated phenyl ring involved in the intrachain π−π stacking as showed above. Furthermore, this pyrazolyl ring participates in a C−H···F hydrogen bond, see Figure 2 (a).

The non-equivalent chains of **1** are organized into a 3-D supramolecular structure by C−H···π interactions. The chains are organized into corrugated sheets by two interactions of this type, with phenyl rings acting as both donors and acceptors. The sheets are situated in the *ab* plane of the crystal. Further, the sheets are held together by another C−H···π interaction, with a pyrazolyl ring acting as donor and a phenyl ring acting as acceptor. The metrical parameters for these interactions are given in Table 2 and are represented by red dotted lines in Figure 3, which shows partial views of two of the sheets down the polymer chains.

Compound **2** is also a coordination polymer, built by the same κ^2−κ^1 coordination mode of the HC(3-Phpz)$_3$ ligand. Figure 4 (a) shows a portion of this coordination polymer together with the partial numbering scheme (for a full crystallographic numbering scheme see the ORTEP representation of **2** in the Supplementary Information, Figure S3). Selected bond lengths and angles are summarized in Table 1. The polyhedra around the silvers are again flattened trigonal pyramids [sum of the N−Ag−N bond angles = 339° for Ag(1) and 343° for Ag(2)], with a large distortion caused by the restricted bite angle [86.08(9)° for Ag(1) and 85.17(9)° for Ag(2)] of the κ^2-bonded ligand. The difference between **1** and **2** is that in **2** there is only one independent chain containing two independent silver atoms, while in **1** there are two independent chains, associated with two independent silver atoms. A similarity with **1** is that the BF_4^- anions are located along the polymeric strand in the vicinity of silver atoms, leading to close contacts between the silver and fluorine atoms along the chain. The Ag···F distances (blue dotted lines) are listed in Table 2, together with other non-covalent parameters for **2**. Another similarity between **1** and **2** is that the BF_4^- anions are not involved in the organization of the supramolecular structure and all the C−H···F weak hydrogen bonds are intrastrand. They are pictured in Figure 4 (a) as blue dotted lines and their metrical parameters are given in Table 2.

In the case of **2** there are several additional non-covalent interactions within the polymeric strands, also represented

Table 2. Non-covalent interactions present in **1**−**4**

	H−A	D−A	D−H−A	Role
1				
Ag(1)−F(1)	2.604(3)	−	−	Intrastrand, secondary bond
Ag(1)−F(2)	3.124(4)	−	−	Intrastrand, secondary bond
Ag(2)−F(5)	2.578(3)	−	−	Intrastrand, secondary bond
C(1)−H(1)−F(1)	2.02	3.00	167.6	Intrastrand, no organization function
C(2)−H(2)−F(5)	2.35	3.30	159.8	Intrastrand, no organization function
C(11)−H(11)−F(3)	2.44	3.34	158.9	Intrastrand, no organization function
C(31)−H(31)−F(2)	2.25	3.00	135.4	Intrastrand, no organization function
C(51)−H(51)−F(8)	2.33	3.13	142.3	Intrastrand, no organization function
C(16)−H(16) − Ct	2.61	3.55	169.5	Organize the strands in sheets
C(36)−H(36) − Ct	2.94	3.76	144.9	Organize the strands in sheets
C(42)−H(42) − Ct	2.66	3.46	142.2	Organize the sheets in 3D
2				
Ag(1)−F(1)	2.761(3)	−	−	Intrastrand, secondary bond
Ag(1)−F(2)	2.988(3)	−	−	Intrastrand, secondary bond
Ag(2)−F(5)	2.481(3)	−	−	Intrastrand, secondary bond
C(1)−H(1)−F(5)	2.31	3.28	165.1	Intrastrand, no organization function
C(2)−H(2)−F(1)	2.09	3.06	160.3	Intrastrand, no organization function
C(21)−H(21)−F(8)	2.30	3.20	157.9	Intrastrand, no organization function
C(51)−H(51)−F(4)	2.24	3.18	174.8	Intrastrand, no organization function
C(37)−H(37) − Ct	2.71 (2.68)	3.60	154.6	Formation of dimers
C(46)−H(46) − Ct	2.67 (2.59)	3.51	147.2	Formation of dimers
C(57)−H(57) − Ct	2.83 (2.82)	3.65	145.8	Organize the dimers into sheets
3				
C(101) − H(101) − F(8)	2.33	3.23	150.1	Formation of Ag(1) chains
C(138) − H(138) − F(5)	2.39	3.24	148.4	Formation of Ag(1) chains
C(201) − H(201) − F(2)	2.04	3.02	166.3	Organize the Ag(2) dimers into sheets
C(211) − H(211) − F(3)	2.28	3.23	172.1	Organize the Ag(2) dimers into sheets
C(238) − H(238) − F(4)	2.45	3.40	172.9	Organize the Ag(2) dimers into sheets
C(222) − H(222) − F(1)	2.45	3.31	150.8	Organize the Ag(2) dimers into sheets
C(143) − H(14E) − F(1)	2.26	3.22	165.3	Support the 3D architecture
C(127) − H(127) − Ct	2.81 (2.73)	3.47	127.7	Organize the Ag(1) chains into sheets
C(217) − H(217) − Ct	2.90 (2.84)	3.75	148.6	Formation of Ag(2) dimers
C(115) − H(115) − Ct	2.90 (2.85)	3.78	152.9	Support the 3D architecture
4				
C(121) − H(121) − F(3)	2.33	3.04	131.6	Bridges one Ag(1) chain and one Ag(2) dimer
C(201) − H(201) − F(1)	2.38	3.30	152.4	Bridges one Ag(1) chain and one Ag(2) dimer
C(211) − H(211) − F(3)	2.34	3.26	162.3	Bridges one Ag(1) chain and one Ag(2) dimer
C(231) − H(231) − F(2)	2.42	3.21	141.2	Bridges one Ag(1) chain and one Ag(2) dimer
C(116) − H(116) − Ct	2.81 (2.74)	3.43	124.0	Formation of Ag(1) chains
C(135) − H(135) − Ct	2.81 (2.79)	3.56	135.7	Formation of Ag(1) chains
C(126) − H(126) − Ct	2.88 (2.84)	3.66	139.4	Organize the Ag(1) chains into sheets
C(216) − H(216) − Ct	3.02 (2.74)	3.96	171.5	Formation of Ag(2) dimers

in Figure 4 (a). There are two π−π stacking interactions involving both pyrazolyl and phenyl rings. One interaction (shown as black double dotted line) involves one of the κ^2 bonded pyrazolyl ring [N(21)−N(22)−C(21)−C(22)−C(23)] and the phenyl ring associated with one of the κ^1 bonded pyrazolyl ring [containing N(61)] with a perpendicular distance between the rings of 3.73 Å. Another π−π interaction involves the second κ^1 bonded pyrazolyl ring [N(31)−N(32)−C(31)−C(32)−C(33)] and a phenyl ring attached to another κ^2 bonded pyrazolyl ring [containing N(51)] with a perpendicular distance between the rings of 3.63 Å. This interaction is shown in Figure 4 (a) by two black arrows pointing toward where the respective group would be located if more of the strand were shown. There are additional C−H···π interactions within the strand (red dotted lines) with the metrical parameters listed in Table 2.

There is substantial tilting of the pyrazolyl rings from the ideal value of 180°. The torsion angles around the Ag(1) atom are 164°, 144°, and 124° and those around the Ag(2) atom are 170°, 151°, and 118°, respectively. As in **1**, these angles are correlated to the non-covalent interactions within the strand. For example, the Ag(1)−N(11)−N(12)−C(11) angle of 124° is related to a C−H···π interaction formed by the [N(11)−N(12)−C(11)−C(12)−C(13)] ring, acting as acceptor, with one of the phenyl rings involved in the π−π stacking interaction. The associated phenyl ring acts also as the acceptor in another C−H···π interaction where the donor is the [N(41)−N(42)−C(41)−C(42)−

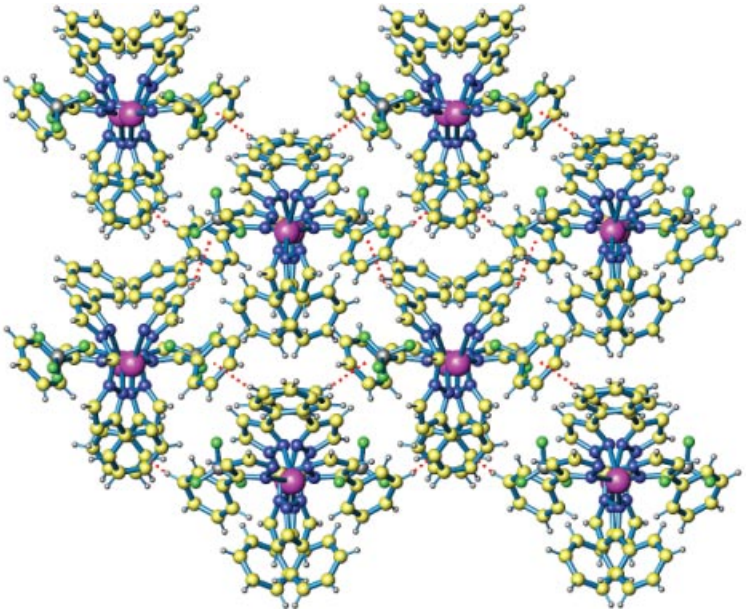

Figure 3. The supramolecular structure of **1** viewed down the *a* axis; the C−H···π interactions that organize the 3-D architecture are shown as red dotted lines

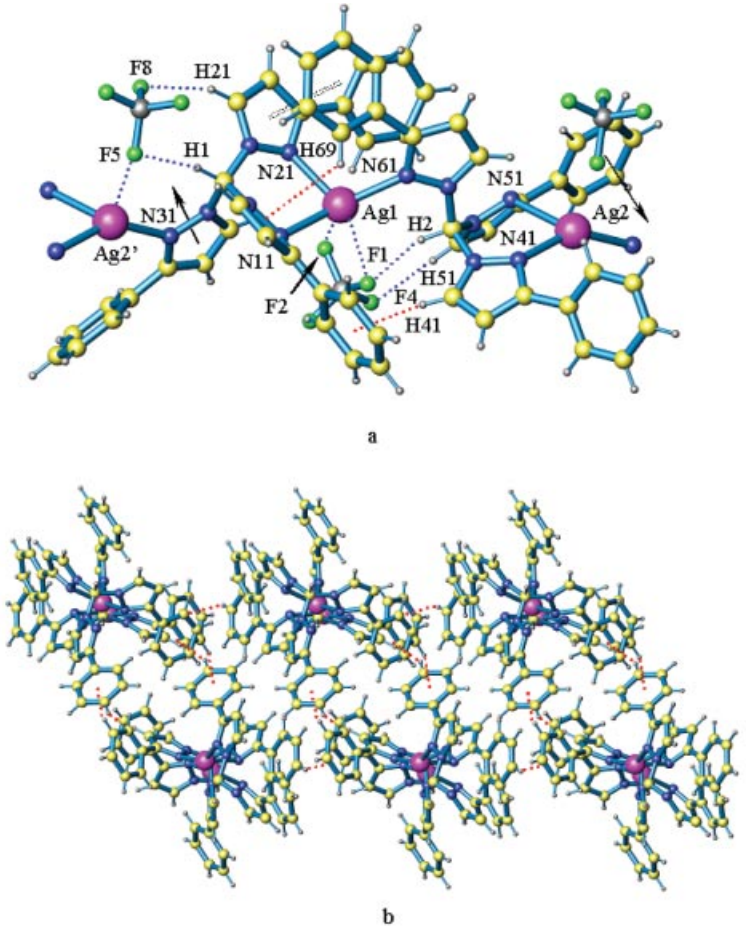

Figure 4. a) Part of the coordination polymer **2**; secondary Ag···F bonds and weak C−H···F hydrogen bonds shown as blue dotted lines and C−H···π interactions as red dotted lines; one π−π stacking is shown as double black dotted lines; the second π−π stacking is pictured by two black arrows. The tilting of the pyrazolyl ring containing N(11) is clearly visible in this orientation; b) formation of the dimeric sheets in **2** via C−H···π interactions, shown as red dotted lines; three dimeric chains are shown, down the *a* axis of the unit cell

C(43)] pyrazolyl ring. The Ag(2)−N(51)−N(52)−C(51) torsion angle of 118° is influenced by four non-covalent interactions. The pyrazolyl ring associated with the largest angle is not involved in any non-covalent interactions.

The supramolecular structure of **2** is only 2-D and is again organized by C−H···π interactions, Table 2. A pair of these interactions organizes the strands into dimers that are oriented in the direction of the *c* axis. A third interaction organizes the dimers into sheets placed parallel to the *ab* plane of the crystal. Figure 4 (b) depicts a 2-D sheet built up from three dimers with the C−H···π interactions represented by red dotted lines.

The replacement of nitromethane with acetone or acetonitrile as the crystallization solvent leads to a dramatic change in the structure of the compound. The coordination of one molecule of solvent to the silver atom, together with a tripodal, κ^3-coordination of the (3-Ph-pyrazolyl)methane ligand leads to the formation of discrete complexes of the formula $[\{HC(3\text{-}Phpz)_3\}Ag\{(CH_3)_2CO\}](BF_4)$ (**3**) and $[\{HC(3\text{-}Phpz)_3\}Ag\{CH_3CN\}](BF_4)$ (**4**).

The crystal structure of **3** contains two symmetry independent units of virtually identical conformation about the silver(I) (see Table 1), but which have different supramolecular contacts. The two units and their partial numbering schemes are represented in Figure 5 (a and b) (for a full crystallographic numbering scheme see the ORTEP representation of **3** in the Supplementary Information, Figure S4; see also footnote on the first page of this article). The silver atoms have a distorted tetrahedral arrangement. For the first unit the average Ag(1)−N distance is 2.37 Å with a corresponding N−Ag(1)−N average angle of 80.64°. The Ag(1)−O distance is 2.231(3) Å, with an average N−Ag(1)−O angle of 131.25°. For the second unit the average Ag(2)−N distance is the same as for the first, 2.37 Å, but with a corresponding N−Ag(2)−N average angle of 81.29°. The Ag(2)−O distance is 2.172(4) Å with the corresponding average N−Ag(2)−O angle of 130.9°.

In contrast with **1** and **2**, where the counterions interacted with the silvers and were not involved in interchain interactions, the cations in **3** are organized into a 3-D structure using both weak C−H···F hydrogen bonds and C−H···π interactions (Table 2). The unit containing the Ag(1) atom is organized into chains via C−H···F hydrogen bonds, Figure 5 (c). The BF_4^- counterion makes two hydrogen bonds, shown as blue dotted lines, one with the methine hydrogen H(101) and another with H(138), a hydrogen situ-

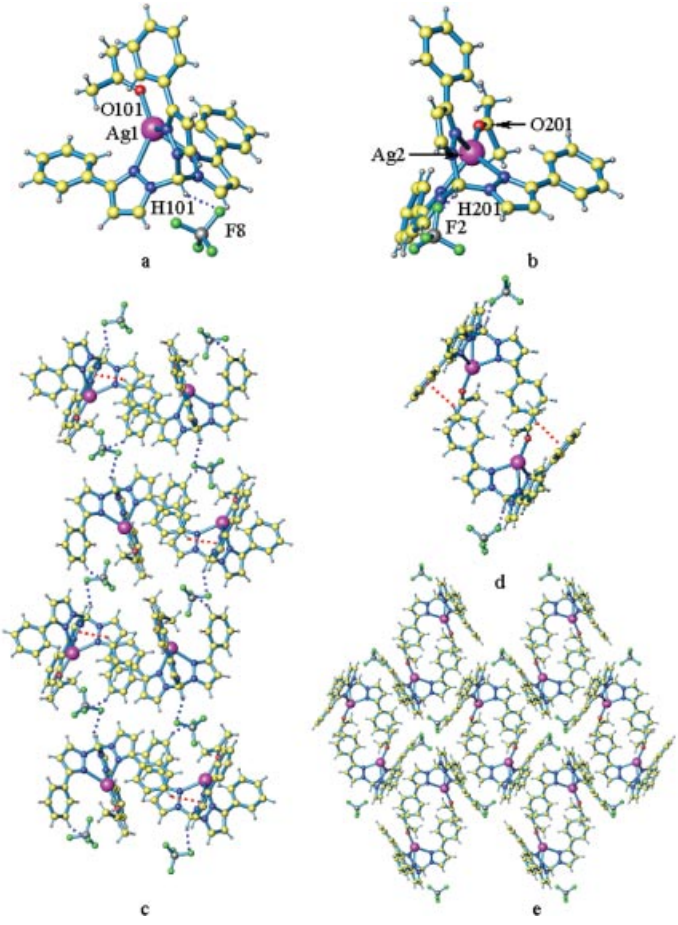

Figure 5. a, b) Two silver(I) building blocks in **3** with their BF_4^- counterions positioned close to the methine hydrogen; color scheme as in Figure 2, plus oxygen red; c) formation of Ag(1) chains and sheets in **3** by the means of C−H···F hydrogen bonds (blue dotted lines) and C−H···π interactions (red dotted lines); d) dimeric association of Ag(2) units, connected by C−H···π interactions, shown as red dotted lines; e) the 2-D network of Ag(2) dimers: view perpendicular to the sheet, showing seven dimers connected by C−H···F weak hydrogen bonds

ated on one of the phenyl rings. The (C)H···F distances to H(101) and H(138) are 2.33 and 2.39 Å with the corresponding C−H−F angles of 150 and 148°. Both these distances are below the sum of van der Waals radii for hydrogen and fluorine[33,34] and are typical for this type of hydrogen bonding.[39,40] These interactions build up chains that run along *c* axis of the unit cell. The chains are arranged into sheets by means of C−H···π interactions, as can be seen also in Figure 5 (c) as red dotted lines. One hydrogen atom from a phenyl group in one cationic unit is pointed toward a pyrazolyl ring within another chain thus generating a sheet in the *bc* plane of the unit cell.

The unit containing the Ag(2) atom has a different supramolecular organization, based again on both C−H···π interactions and weak C−H···F hydrogen bonds. One C−H···π interaction is between H(217), located in a phenyl ring and the pi cloud of a phenyl ring on an adjacent silver(I) unit, Figure 5 (d). The hydrogen to centroid distance is 2.90 Å with the corresponding C−H-centroid angle of 149° see also Table 2. This distance is typical for C−H···π interactions.[36,37] A pair of these interactions, showed as red dotted lines, links two Ag(2) units forming a dimer.

The BF_4^- ions connect these dimers into a 2-D supramolecular network (see Table 2 for metrical parameters) via C−H···F hydrogen bonds. Figure 5 (e) shows seven dimeric assemblies viewed in the same orientation as in Figure 5 (d), connected by the BF_4^- anions. At the corners of each square shaped dimeric unit, each dimer is bonded to four other dimers arranged in a square around it through four BF_4^- anions. The two "outside" dimers in Figure 5 (e) are not connected to the central dimer but to the two dimeric units above and below them in the figure.

The sheets associated with Ag(1) and Ag(2) are arranged in a 3-D architecture again by weak C−H···F hydrogen bonds and C−H···π interactions, Figure 6. One fluorine atom that is part of the BF_4^- anion involved in the organization of the Ag(2) units in chains makes a close contact with a hydrogen located on an acetone molecule coordinated to an Ag(1) unit. The H···F contact is 2.26 Å (C···F contact of 3.22 Å) with a corresponding C−H−F angle of 165°. A second interaction holding the sheets together is a C−H···π interactions formed between a hydrogen atom situated on a phenyl ring within the Ag(1) unit and another phenyl ring that is part of Ag(2) unit. The H···centroid distance is 2.90 Å and the C···centroid distance of 3.78 Å, with the corresponding C−H-centroid angle of 153°.

When acetone was replaced with acetonitrile in the crystallization procedure, the structures of the two silver(I) units of the resulting compound (**4**) are similar to those of **3**. The crystal structure of **4** contains two symmetry independent units of virtually identical conformation but which have different supramolecular contacts. The two units and their partial numbering schemes are represented in Figure 7 (for a full crystallographic numbering scheme see the ORTEP representation of **4** in the Supplementary Information, Figure S5). The silver atoms again have a distorted tetrahedral arrangement. For the first unit the average $Ag(1)-N_{pz}$ distance is 2.36 Å with a corresponding $N_{pz}-Ag-N_{pz}$ average angle of 80.06°. The Ag(1)−N(101) distance is 2.137(2) Å, with an average $N_{pz}-Ag(1)-N(101)$ angle of 132.03°. For the second unit the average $Ag(2)-N_{pz}$ distance is 2.37 Å, with a corresponding $N_{pz}-Ag-N_{pz}$ average angle of 80.78°. The Ag(2) − N(201) distance in this case is 2.149(2) Å with the corresponding average $N_{pz}-Ag(2)-N(201)$ angle of 131.19°. For further details on the bond lengths and angles see Table 1. The BF_4^- counterions make hydrogen bonds with the hydrogen atoms attached to the central methine carbon atoms. The BF_4^- anion associated with Ag(1) was found to be disordered over two closely spaced positions so further discussions about its role in the extended structure of **4** are precluded; Figure 7 (a) pictures one component of the disordered counterion, but in further discussions this counterion will not be mentioned.

The units containing the Ag(1) silver atoms are organized in chains running along the *b* axis by means of two C−H···π interactions (see Table 2 for details). In both cases, two pyrazolyl rings act as acceptors and two phenyl rings as hydrogen donors. Figure 8 (a) illustrates three chains, that are further connected in a 2-D network, again through C−H···π interactions, with pyrazolyl rings acting as acceptors and phenyl rings as hydrogen donors. The interactions responsible for the formation of the chains and sheets are pictured as red dotted lines in Figure 8 (part a). Figure 8 (part b) is a view end-on of the Figure 8 (part a), showing the orientation of the sheets in the *bc* plane of the unit cell.

The units containing the Ag(2) atoms are arranged in a different way. A double π−π/C−H···π interaction organizes these units in dimers, as pictured in Figure 9. The metrical

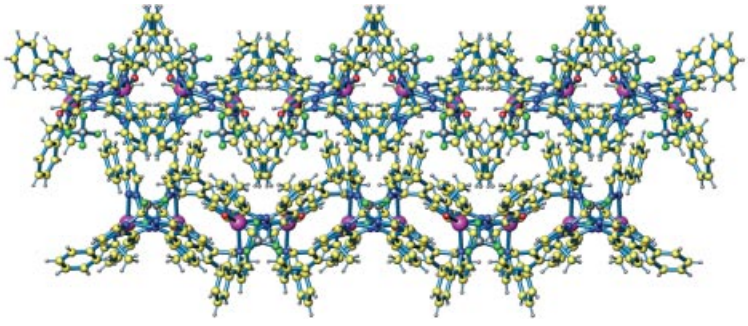

Figure 6. The 3-D architecture of **3** formed by combining the Ag(1) and Ag(2) sheets

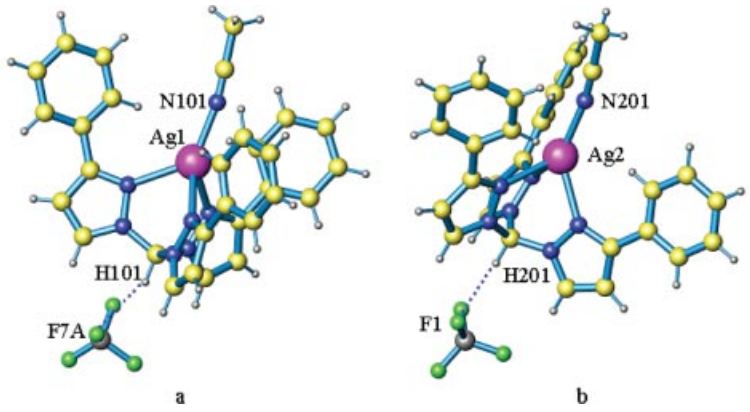

Figure 7. Two silver(I) building blocks in **4** with the BF_4^- counterions positioned close to the methine hydrogen; the BF_4^- anion in (a) is disordered over two positions; only one component is shown here

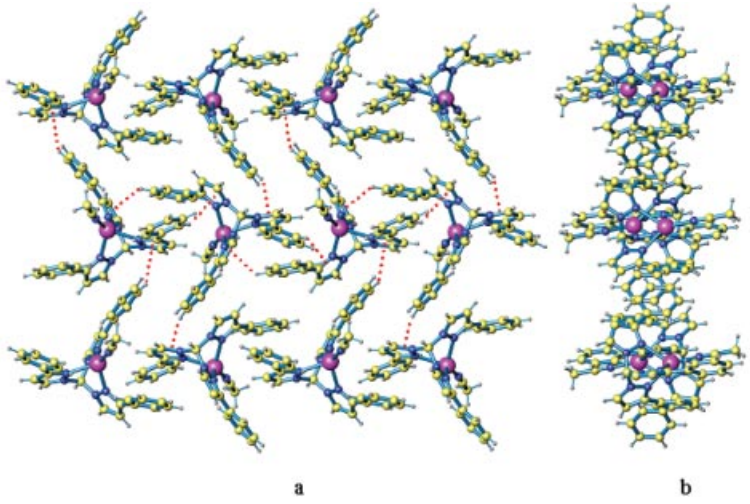

Figure 8. Formation of Ag(1) sheets in **4**: a) view perpendicular to the sheet, illustrating three interconnected chains; the C−H···π interactions that form the chains are represented only within the middle chain; b) end-on view of the same sheet in the *bc* plane of the unit cell

parameters for these non-covalent interactions are listed in Table 2. The π−π stacking is between two phenyl rings that also act as hydrogen donors in the C−H···π interaction, with two other phenyl rings acting as acceptors. The stacked phenyl rings are parallel, but displaced in order to maximize the C−H···π interaction, the angle formed by the centroid−centroid vector with the ring normal being 30°. The centroid−centroid distance is 3.9 Å and the perpendicular distance between the planes is 3.4 Å.[35] There is also a shift from an ideal geometric arrangement for the C−H···π interaction. The presence of the π−π stacking between the parallel displaced phenyl rings leads to a rather long H···centroid distance of 3.02 Å, but the perpendicular distance from the hydrogen atom to the acceptor phenyl planes is 2.7 Å, with the corresponding C−H−centroid angle of 171°.[36,37]

These two units are arranged into a supramolecular structure by the means of weak (C)H···F hydrogen bonds. The ordered BF_4^- counterion act as a bridge between one Ag(1) chain and one Ag(2) dimer, Figure 10 (a). The F(3) atom within the BF_4^- counterion is involved in a bifurcated hydrogen bond with two hydrogen atoms located on the fifth carbon atom of the pyrazolyl rings. As it can be seen in Table 2, the H···F contacts are short, with C−H−F angles approaching to linearity. The resultant architecture is further connected into a 3-D network by the non-covalent C−H···π interactions that connects the Ag(1) chains into sheets, as pictured in Figure 10 (b). There is no non-coval-

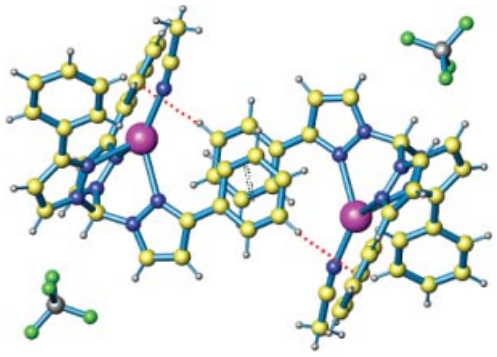

Figure 9. Dimeric association of Ag(2) building blocks in **4** via a double π−π stacking (black double dotted line)/C−H···π (red dotted lines) interaction

ent interaction holding the dimers associated with Ag(2) together. The sheets in Figure 10 (b) are in the same orientation as in Figure 8 (b).

Comparison of Molecular and Supramolecular Structures

Our systematic X-ray crystallographic studies reveal that a coordinating solvent dramatically changes the molecular structures and/or the supramolecular structures of the four forms of [{HC(3-Phpz)$_3$}Ag](BF_4) studied here. In the absence of a coordinating solvent, the tris(3-phenyl-pyrazolyl)methane ligand bridges two silver atoms in the κ^2-κ^1 bonding mode forming coordination polymers arranged in argentachains. This arrangement of the ligands allows room for the BF_4^- counterion to be located in the vicinity of the silver atoms, with close silver−fluorine contacts (see Table 2 and Figure 2, a, b and Figure 4, a). This secondary interaction between the silver and fluorine atoms completes the fourth coordination site and prevents the anions from participating in the organization of the subsequent supramolecular structures of the polymeric chains. Two polymorphs with the same basic κ^2-κ^1 coordinating mode have been crystallized that have different supramolecular structures based on similar types of non-covalent interactions. In compound **1** there are two independent chains having different shapes (Figure 2, d and f) and in **2** only one type of chain is present, with a different internal structure than in **1**. Noncovalent forces organize the chains into sheets and the sheets into a final 3-D supramolecular structure in the case of **1**, while in the case of **2** only a 2-D supramolecular structure forms (compare Figures 3 and 4, b).

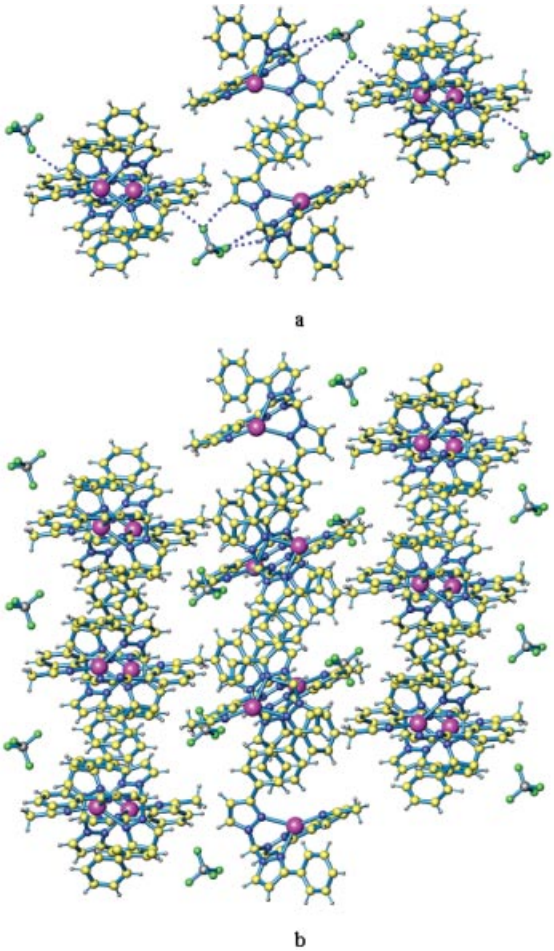

Figure 10. a) Two Ag(1) chains and one Ag(2) dimer in **4** bridged by the counterions, with the C−H···F hydrogen bonds shown as blue dotted lines; one fluorine atom makes a bifurcated hydrogen bond with hydrogen atoms situated on the fifth position of pyrazolyl rings; b) the extended 3-D structure of **4**, showing six Ag(1) chains in two Ag(1) sheets (left and right, view down the chains) and three Ag(2) dimers (middle) bridged by six BF_4^- counterions

The structures of the same complex crystallized from the coordinating solvents acetone and acetonitrile are very different from **1** and **2**. The structures feature a κ^3 tripodal coordination mode of the tris(3-phenylpyrazolyl)methane ligand with the fourth coordination site on the silver filled with the solvent, thus generating the discrete compounds **3** (Figure 5, a, b) and **4** (Figure 7) rather than coordination polymers. In both cases the structures of the silver cationic units are very similar. Their asymmetric units contain two chemically similar but crystallographically independent [HC(3-Phpz)$_3$Ag(solvent)] cations. The coordination environment around the silver atom is also similar − a distorted tetrahedron.

The supramolecular structures of **3** and **4** are also similar. In both cases one type of silver(I) unit associates in chains and then in sheets (Figure 5, c, and Figure 8). The second type of silver(I) forms dimeric units (Figure 5, d, and Figure 9). Association between the sheets and dimers leads in both cases to a 3-D supramolecular structure. However, the connection pattern and the resulting extended structures are different. In the case of **3** the chains are supported by weak H···F hydrogen bonds with the BF_4^- counterion acting as a bridge between the cationic units, whereas in **4** the chains are formed only by the means of C−H···π interactions with phenyl rings acting as hydrogen donors and pyrazolyl rings acting as acceptors. The sheets that result from the association of the chains are in both cases supported by C−H···π interactions where the phenyl rings are the donors and pyrazolyl rings are the acceptors.

The mode of formation of the dimeric units in each structure is also different. The self-assembly of the dimeric units in **3** are supported by C−H···π interactions with phenyl rings acting as hydrogen donors and acceptors, while in **4** there is an additional π−π stacking between the phenyl rings that are the hydrogen donors in the C−H···π interaction. The shape of the acetone molecule (two methyl groups, see Figure 5, d) prevents the donor phenyl rings involved in the C−H···π interaction from getting close enough for the additional π−π stacking observed in the case of **4**, where an acetonitrile molecule (one methyl group, see Figure 9) does not have such a pronounced steric effect.

The role of the dimers is also different. In **3**, the dimers are arranged in chains by the non-covalent forces, forming a 2-D array of dimers (Figure 5, e) and the association of these sheets forms the overall supramolecular structure pictured in Figure 6. In contrast, in **4** the dimers are not arranged into an extended structure, their contribution to the 3-D supramolecular structure is that they act, together with the BF_4^- anions, as a bridge between two sheets, as shown in Figure 10 (a).

Conclusion

An important conclusion of this work is that in silver(I) chemistry the non-linked, tris(pyrazolyl)methane ligand HC(3-Phpz)$_3$ supports complex supramolecular structures using the same types of covalent and non-covalent forces observed in the silver(I) complexes of the linked multitopic ligands studied earlier. In the absence of a coordinating solvent, [{HC(3-Phpz)$_3$}Ag](BF$_4$) forms two polymorphs with structures dominated by polymeric argentachains that are constructed from the κ^2-κ^1 bonding mode of each ligand, a bonding mode that is frequently observed in the structures of the linked ligands.[20,21,25] In these structures, the weakly coordinating counterion BF_4^- bonds to the silvers completing the coordination spheres. This interaction removes the BF_4^- groups from the ability to support the supramolecular structure through weak H···F hydrogen bonds with the acid hydrogen atoms located on the ligands of different cationic units.

When [{HC(3-Phpz)$_3$}Ag](BF$_4$) is crystallized from coordinating solvents, the solvent bonds directly to silver. The presence of the coordinating solvent changes the bonding mode of the HC(3-Phpz)$_3$ ligand to tripodal. Even in the absence of a coordination polymer formed by either the κ^2-κ^1 coordinating mode or from the linking component of the multitopic ligands, complex supramolecular structures form from an interesting array of non-covalent interactions. In these structures, the BF_4^- does not interact with the metal, but contributes to the supramolecular structures through weak H···F hydrogen bonds.

Tris(pyrazolyl)methane ligands, whether monotopic or multitopic, clearly contain functionality that supports 2D and 3D supramolecular structures organized by weak hydrogen bonds, π−π stacking, and C−H···π interactions. Their ability to act as (a) κ^3 tripodal, (b) κ^2 bonded to a single metal with the third pyrazolyl not coordinated, and (c) κ^2-κ^1 bonded bridging two metals adds to the structural diversity observed for silver(I) complexes of these ligands. The 3-phenyl substituents on the pyrazolyls add to the structural diversity of HC(3-Phpz)$_3$ complexes in comparison to those of the parent HC(pz)$_3$ ligand.

An understanding of how the covalent and non-covalent forces organize the supramolecular self-assembly process is a prerequisite for the progress of crystal engineering. This study shows that although the same types of forces are involved in building the supramolecular structures of **1**−**4**, differences were found when the extended structures of even similar building blocks were compared. A good example is given by the formation of the dimeric units of **3** and **4** and their role in the extended structures. In one case they are formed only by a C−H···π interaction and in the other there is an additional π−π stacking as a supporting interaction. Also, each has a different role in the resulting supramolecular structure. Further studies are clearly needed in order to ascertain the influence of *all* factors on the outcome of a supramolecular arrays if one hopes to fully understand/control the self-assembly process.

Experimental Section

General Remarks: All manipulations involving uncomplexed silver tetrafluoroborate were carried out either in a Vacuum Atmospheres HE-493 dry box under a N_2 atmosphere or by using standard

Schlenk techniques. After complexation of the silver salt by the ligand no precautions were taken to exclude moisture or oxygen. All solvents were dried using conventional procedures and distilled prior to use. The ^{1}H NMR spectra were recorded on a Varian AM300 spectrometer using a broad-band probe. Proton chemical shifts are reported in ppm vs. internal Me_4Si. Mass spectroscopic data were recorded on a MicroMass QTOF spectrometer. Clusters assigned to specific ions show appropriate isotopic patterns as calculated for the atoms present. Robertson Microlit Laboratories, Inc. (Madison, NJ) performed the elemental analyses. Silver tetrafluoroborate and 3-Ph-pyrazole (3-PhpzH) were used as purchased from Aldrich. Samples for melting point determinations were contained in flame sealed capillaries and the reported temperatures are uncorrected.

HC(3-Phpz)$_3$: Distilled water (400 mL) was added to a 1000 mL flask containing a mixture of 3-phenylpyrazole (28.8 g, 0.20 mol) and tetra-*n*-butylammonium bromide (3.2 g, 9.9 mmol). With vigorous stirring, sodium carbonate (127 g, 1.2 mol) was added gradually to the reaction mixture. Then chloroform (150 mL) was added and the flask was equipped with a reflux condenser. This mixture was heated at reflux for 3 days over which time it became a dark yellow emulsion. The mixture was allowed to cool to room temp. and filtered to remove the solid Na_2CO_3. The organic layer was separated from the aqueous layer and the latter extracted with diethyl ether (3 × 75 mL). The combined organic layers were washed with distilled water (2 × 150 mL) and dried over sodium sulfate. The solution was filtered and the solvent was removed by rotary evaporation. The resulting off-white solid containing 3/5-substituted isomers was then dissolved in the minimum required amount of boiling toluene and poured into a 100 mL flask containing a small amount of *p*-toluenesulfonic acid monohydrate (ca. 0.1 g). The golden solution was heated at reflux temperature overnight. After it had cooled to room temp., an off-white precipitate appeared that was filtered with suction. The moist powder was taken into a beaker and 200 mL of distilled water added. After 2 hours of stirring the suspension was filtered (suction), washed twice with water and once with hexanes, to afford 15 g (52%) of pure HC(3-Phpz)$_3$ as a white powder. M.p. 125−126 °C. ^{1}H NMR ([D$_6$]acetone): δ = 8.86 (s, 1 H, *H*C), 8.10 (d, *J* = 2.1 Hz, 3 H, 5-H *pz*), 7.90 (m, 6 H, *o*-H *Ph*), 7.42 (m, 6 H, *m*-H *Ph*), 7.35 (m, 3 H, *p*-H *Ph*), 6.90 (d, *J* = 2.1 Hz, 3 H, 4-H *pz*) ppm. ^{1}H NMR ([D$_3$]nitromethane): δ = 8.64 (s, 1 H, *H*C), 7.95 (d, *J* = 2.7 Hz, 3 H, 5-H *pz*), 7.87 (m, 6 H, *o*-H *Ph*), 7.42 (m, 9 H, *m*-H, *p*-H *Ph*), 6.86 (d, *J* = 2.7 Hz, 3 H, 4-H *pz*) ppm.

[{HC(3-Phpz)$_3$}Ag](BF$_4$): *Reaction A (1:1 metal to ligand ratio):* Silver tetrafluoroborate, $AgBF_4$ (0.195 g, 1.0 mmol) was dissolved in dry THF (15 mL). To this solution was added via syringe a solution of HC(3-Phpz)$_3$ (0.442 g, 1.0 mmol) in THF (15 mL). After stirring the reaction mixture overnight, hexanes were added (75 mL) and a white precipitate appeared. The mixture was kept 1 hour at −20 °C, and then quickly filtered to afford 0.592 g (93%) of a white powder identified by elemental analysis as [{HC(3-Phpz)$_3$}Ag](BF$_4$): $C_{28}H_{22}AgBF_4N_6$ calcd. C 52.79, H 3.45, N 13.18%, found C 52.43, H 3.65, N 13.09%. *Reaction B (1:2 metal to ligand ratio):* The second procedure involved the same steps as procedure A, using 0.097 g of $AgBF_4$ (0.50 mmol) and 0.442 g of HC(3-Phpz)$_3$ (1.0 mmol). The white compound obtained was identified by elemental analysis as [{HC(3-Phpz)$_3$}Ag](BF$_4$): $C_{28}H_{22}AgBF_4N_6$ calcd. C 52.79, H 3.45, N 13.18, found C 52.93, H 3.36, N 12.79. In addition, 0.5 mol of the ligand was recovered from the filtrate. The ^{1}H NMR spectra of the two samples were identical and they are listed below [D$_6$]acetone: δ = 9.30 (s, 1 H, *H*C), 8.42 (d, *J* = 2.4 Hz, 3 H, 5-H *pz*), 7.92 (m, 6 H, *o*-H *Ph*), 7.43 (m, 9 H, *m*-H, *p*-H *Ph*), 6.98 (d, *J* = 2.4 Hz, 3 H, 4-H *pz*) ppm; [D$_3$] nitromethane: δ 8.67 (s, 1 H, *H*C), 8.19 (d, *J* = 2.4 Hz, 3 H, 5-H *pz*), 7.83 (m, 6 H, *o*-H *Ph*), 7.41 (m, 9 H, *m*-H, *p*-H *Ph*), 6.87 (d, *J* = 2.7 Hz, 3 H, 4-H *pz*) ppm.

X-ray Crystallographic Study: Suitable colorless single crystals of **1**−**4** were selected and mounted onto thin glass fibers. Low-temperature X-ray intensity data were measured on a Bruker SMART APEX CCD-based diffractometer (Mo-*Kα* radiation, λ = 0.71073 Å). After preliminary crystal quality and unit cell parameter determination, a full sphere (**1**, **2**) or hemisphere (**3**, **4**) of raw frame data was collected. Raw data frame integration was performed with SAINT+,[41] which also applied corrections for Lorentz and polarization effects. Analysis of each data set showed negligible crystal decay during data collection. Empirical absorption corrections were applied to each data set (SADABS)[41] in the case of **1**, **2**, and **4**, while in the case of **3** no correction for absorption was applied. The reported final unit cell parameters are based on the least-squares refinement of all reflections from each data set with $I > 5\sigma(I)$. The structures were solved by a combination of direct methods and difference Fourier syntheses and refined by full-matrix least-squares against F^2 (SHELXTL).[42] Non-hydrogen atoms in each structure were refined with anisotropic displacement parameters; hydrogen atoms were placed in idealized positions and included as riding atoms. For **1** systematic absences in the intensity data were consistent with the space groups *Pcam* and *Pca*2$_1$; intensity statistics indicated acentricity. The structure was solved in the polar space group *Pca*2$_1$. Upon successful solution and refinement in *Pca*2$_1$, a check for missed symmetry using the ADDSYM program in PLATON[43] verified the space group choice. All atoms reside on positions of general crystallographic symmetry. The structure contains two crystallographically independent polymeric chains, associated with the independent atoms Ag(1) and Ag(2). At the end of the refinement, the Flack parameter was 0.24(2), indicating that both orientations of the polar axis are present and the crystal is an inversion twin. Refinement of the data accounting for the twinning[42] yielded twin fractions of 0.76/0.24. Compound **2** crystallizes in the triclinic system. The space group $P\bar{1}$ was assumed and confirmed by the successful solution and refinement of the structure. The asymmetric unit contains two ligands, two silver atoms and two BF_4^- counterions with all of them residing on positions of general crystallographic symmetry. Systematic absences in the data sets for **3** and **4** were consistent with the space group $P2_1/c$, and the structures were readily solved in this space group. The asymmetric unit of **3** contains two chemically similar but crystallographically independent [{HC(3-Phpz)$_3$Ag}(CH$_3$)$_2$CO]$^+$ cations, two BF_4^- anions and one acetone molecule of crystallization. All atoms reside on positions of general crystallographic symmetry. The asymmetric unit of **4** contains two chemically similar but crystallographically independent [{HC(3-Phpz)$_3$Ag}(CH$_3$CN)]$^+$ cations, two BF_4^- anions, and one diethyl ether molecule of crystallization. All atoms reside on positions of general crystallographic symmetry. One BF_4^- anion is disordered over two closely spaced positions; a total of 30 geometric restraints (SHELX SAME) were used to assist in modeling the disorder. Crystal data and structure refinement for all compounds are presented in Table 3. CCDC 203781−203784 (**1**−**3**) and -205526 (**4**) contains the supplementary crystallographic data for this paper. These data can be obtained free of charge at www.ccdc.cam.ac.uk/conts/retrieving.html [or from the Cambridge Crystallographic Data Centre, 12, Union Road, Cambridge CB2 1EZ, UK; fax: (internat.) +44-1223/336-033; E-mail: deposit@ccdc.cam.ac.uk].

Table 3. Crystal data and structure refinement for **1**−**4**

	1	**2**	**3**	**4**
Empirical formula	$C_{28}H_{22}AgBF_4N_6$	$C_{28}H_{22}AgBF_4N_6$	$C_{32.50}H_{31}AgBF_4N_6O_{1.50}$	$C_{32}H_{30}AgBF_4N_7O_{0.50}$
Molecular mass	637.20	637.20	724.31	715.31
Temperature [K]	150.0(2)	150.0(2)	190(2)	173(2)
Wavelength	0.71073	0.71073	0.71073 Å	0.71073 Å
Crystal system	Orthorhombic	Triclinic	Monoclinic	Monoclinic
Space group	$Pca2_1$	$P\bar{1}$	$P2_1/c$	$P2_1/c$
a [Å]	14.3467(7)	12.3992(6)	19.1516(11)	21.7605(9)
b [Å]	15.7777(8)	13.9575(7)	16.2130(10)	15.9462(7)
c [Å]	24.1775(12)	16.4625(8)	21.3959(13)	18.7512(8)
α [deg]	90°	93.2900(10)	90°	90°
β [deg]	90°	95.2510(10)	105.6890(10)	99.2920(10)
γ [deg]	90°	109.9850(10)	90°	90°
V [Å^3]	5472.8(5)	2654.2(2)	6396.0(7)	6421.2(5)
Z	8	4	8	8
Density (calcd.) [Mg·m^{-3}]	1.547	1.595	1.504	1.480
Absorption coefficient [mm^{-1}]	0.793	0.818	0.692	0.687
F(000)	2560	1280	2944	2904
Crystal size [mm]	0.40 × 0.26 × 0.14	0.56 × 0.10 × 0.04	0.28 × 0.24 × 0.16	0.56 × 0.42 × 0.40
Reflections collected	48614	24621	42399	46296
Independent reflections	11181[R(int) = 0.0408]	10827[R(int) = 0.0350]	13102 [R(int) = 0.0545]	13149 [R(int) = 0.0484]
Data/restraints/parameters	11181/1/722	10827/0/721	13102/2/835	13149/30/861
Goodness-of-fit on F^2	1.033	1.011	0.943	1.013
Final *R* indices [$I > 2\sigma(I)$]	$R1 = 0.0346, wR2 = 0.0762$	$R1 = 0.0418, wR2 = 0.0899$	$R1 = 0.0494, wR2 = 0.1001$	$R1 = 0.0340, wR2 = 0.0742$
R indices (all data)	$R1 = 0.0375, wR2 = 0.0774$	$R1 = 0.0565, wR2 = 0.0993$	$R1 = 0.0854, wR2 = 0.1090$	$R1 = 0.0473, wR2 = 0.0777$

Acknowledgments

We thank the National Science Foundation (CHE-0110493) for support. The Bruker CCD Single Crystal Diffractometer was purchased using funds provided by the NSF Instrumentation for Materials Research Program through Grant DMR:9975623.

[1] S. Trofimenko, *J. Am. Chem. Soc.* **1966**, *88*, 1842.
[2] S. Trofimenko, *Scorpionates: The Coordination Chemistry of Polypyrazolylborate Ligands*, Imperial College Press, London, 1999.
[3] F. T. Edelman, *Angew. Chem.* **2001**, *113*, 1704; *Angew. Chem. Int. Ed.* **2001**, *40*, 1656.
[4] C. Janiak, S. Temizdemir, S. Dechert, *Inorg. Chem. Commun.* **2000**, *3*, 271.
[5] M. M. Diaz-Requejo, T. R. Belderrain, M. C. Nicasio, P. J. Perez, *Organometallics* **2000**, *19*, 285.
[6] N. Kitajima, Y. Moro-oka, *Chem. Rev.* **1994**, *94*, 737.
[7] G. Parkin, *Adv. Inorg. Chem.* **1995**, *42*, 291.
[8] H. Vahrenkamp, *Acc. Chem. Res.* **1999**, *32*, 589.
[9] A. M. Santos, F. E. Kuhn, K. Bruus-Jensen, I. Lucas, C. C. Romao, E. Herdtweck, *J. Chem. Soc., Dalton Trans.* **2001**, 1332.
[10] D. L. Reger, *Comment, Inorg. Chem.* **1999**, *21*, 1.
[11] D. L. Reger, J. E. Collins, A. L. Rheingold, L. M. Liable-Sands, G. P. A. Yap, *Organometallics* **1996**, *15*, 2029.
[12] D. L. Reger, J. E. Collins, A. L. Rheingold, L. M. Liable-Sands, G. P. A. Yap, *Organometallics* **1997**, *16*, 349.
[13] D. L. Reger, T. C. Grattan, K. J. Brown, C. A. Little, J. J. S. Lamba, A. L. Rheingold, R. D. Sommer, *J. Organomet. Chem.* **2000**, *607*, 120.
[14] D. L. Reger, C. A. Little, M. D. Smith, A. L. Rheingold, L. M. Liable-Sands, G. P. A. Yap, L. A. Guzei, *Inorg. Chem.* **2002**, *41*, 19.
[15] D. L. Reger, C. A. Little, M. D. Smith, G. J. Long, *Inorg. Chem.* **2002**, *41*, 4453.
[16] A. Cingolani, M. D. Effendy, M. Pellei, C. Pettinari, B. W. Skelton, A. H. White, *Inorg. Chim. Acta* **2002**, *328*, 87.
[17] D. A. McMorran, P. J. Steel, *Inorg. Chem. Commun.* **2003**, *6*, 43.
[18] D. A. McMorran, S. Pfadenhauer, P. J. Steel, *Aust. J. Chem.* **2002**, *55*, 519.
[19] D. L. Reger, T. D. Wright, R. F. Semeniuc, T. C. Grattan, M. D. Smith, *Inorg. Chem.* **2001**, *40*, 6212.
[20] D. L. Reger, R. F. Semeniuc, M. D. Smith, *Inorg. Chem.* **2001**, *40*, 6545.
[21] D. L. Reger, R. F. Semeniuc, M. D. Smith, *Eur. J. Inorg. Chem.* **2002**, 543.
[22] D. L. Reger, R. F. Semeniuc, M. D. Smith, *J. Chem. Soc., Dalton Trans.* **2002**, 476.
[23] D. L. Reger, R. F. Semeniuc, M. D. Smith, *Inorg. Chem. Commun.* **2002**, *5*, 278.
[24] D. L. Reger, R. F. Semeniuc, M. D. Smith, *J. Organomet. Chem.* **2003**, *666*, 87.
[25] D. L. Reger, R. F. Semeniuc, M. D. Smith, *Dalton Trans.* **2003**, 285.
[26] A. N. Khlobystov, A. J. Blake, N. R. Champness, D. A. Lemenovskii, G. Majouga, N. V. Zyk, M. Schröder, *Coord. Chem. Rev.* **2001**, *222*, 155.
[27] A. J. Blake, N. R. Champness, P. Hubberstey, W.-S. Li, M. A. Withersby, M. Schröder, *Coord. Chem. Rev.* **1999**, *183*, 117.
[28] D. L. Reger, R. F. Semeniuc, M. D. Smith, *Rev. Roumaine Chim.* **2002**, *47*, 1035.
[29] D. L. Reger, K. J. Brown, M. D. Smith, *J. Organomet. Chem.* **2002**, *658*, 50.
[30] S. B. Seymore, S. N. Brown, *Inorg. Chem.* **2000**, *39*, 325.
[31] K. A. Hirsch, S. R. Wilson, J. S. Moore, *J. Am. Chem. Soc.* **1997**, *119*, 10401.
[32] N. W. Alcock, R. M. Countryman, *J. Chem. Soc., Dalton Trans.* **1977**, 217.
[33] A. Bondi, *J. Phys. Chem.* **1964**, *68*, 441.
[34] R. S. Rowland, R. Taylor, *J. Phys. Chem.* **1996**, *100*, 738.

[35] C. Janiak, *J. Chem. Soc., Dalton Trans.* **2000**, 3885 and references cited therein.
[36] M. Nishio, M. Hirota, Y. Umezawa, *The CH/π interaction Evidence, Nature and Consequences*, Wiley-VCH, New York, **1998**.
[37] H. Takahashi, S. Tsuboyama, Y. Umezawa, K. Honda, M. Nishio, *Tetrahedron* **2000**, *56*, 6185.
[38] D. L. Reger, T. D. Wright, C. A. Little, J. J. S. Lamba, M. D. Smith, *Inorg. Chem.* **2001**, *40*, 3810.
[39] V. R. Thalladi, H. C. Weiss, D. Blaser, R. Boese, A. Nangia, G. R. Desiraju, *J. Am. Chem. Soc.* **1998**, *120*, 8702.
[40] F. Grepioni, G. Cojazzi, S. M. Draper, N. Scully, D. Braga, *Organometallics* **1998**, *17*, 296.
[41] *SMART* Version 5.625, *SAINT+* Version 6.02a, and *SADABS*. Bruker Analytical X-ray Systems, Inc., Madison, Wisconsin, USA, **1998**.
[42] G. M. Sheldrick, *SHELXTL* Version 5.1; Bruker Analytical X-ray Systems, Inc., Madison, Wisconsin, USA, **1997**.
[43] A. L. Spek, *PLATON*, A Multipurpose Crystallographic Tool, Utrecht University, Utrecht, The Netherlands, **2003**.

Received March 13, 2003

